

NASA Technical Memorandum 106066
AIAA-92-3108

1N-20

160259

P.18

Measurement and Analysis of a Small Nozzle Plume in Vacuum

P.F. Penko
*Lewis Research Center
Cleveland, Ohio*

I.D. Boyd
*Eloret Institute
Ames Research Center
Moffett Field, California*

and

D.L. Meissner and K.J. DeWitt
*University of Toledo
Toledo, Ohio*

Prepared for the
28th Joint Propulsion Conference and Exhibit
cosponsored by the AIAA, SAE, ASME, and ASEE
Nashville, Tennessee, July 6-8, 1992

NASA

(NASA-TM-106066) MEASUREMENT AND
ANALYSIS OF A SMALL NOZZLE PLUME IN
VACUUM (NASA) 18 p

504616

N93-26561

Unclas

22p

G3/20 0160259



MEASUREMENT AND ANALYSIS OF A SMALL NOZZLE PLUME IN VACUUM

P.F. Penko[†]
NASA Lewis Research Center,
Cleveland, OH

I.D. Boyd[‡]
Eloret Institute,
NASA Ames Research Center,
Moffett Field, CA

D.L. Meissner^{*} and K.J. DeWitt[§]
University of Toledo,
Toledo, OH

Abstract

Pitot pressures and flow angles are measured in the plume of a nozzle flowing nitrogen and exhausting to a vacuum. Total pressures are measured with Pitot tubes sized for specific regions of the plume and flow angles measured with a conical probe. The measurement area for total pressure extends 480 mm (16 exit diameters) downstream of the nozzle exit plane and radially to 60 mm (1.9 exit diameters) off the plume axis. The measurement area for flow angle extends to 160 mm (5 exit diameters) downstream and radially to 60 mm. The measurements are compared to results from a numerical simulation of the flow that is based on kinetic theory and uses the direct-simulation Monte Carlo (DSMC) method. Comparisons of computed results from the DSMC method with measurements of flow angle display good agreement in the far-field of the plume and improve with increasing distance from the exit plane. Pitot pressures computed from the DSMC method are in reasonably good agreement with experimental results over the entire measurement area.

Introduction

NASA has a continuing effort in developing small rockets that operate on electrical power for both primary and auxiliary satellite propulsion. These rockets are typified by thrusts of order 1 N or less and by nozzle flows that can be quite viscous. An important consideration in using such thrusters is the effect that the plumes may have on various satellite systems and functions. Given the viscous nature of the flow in these thrusters, the plumes tend to spread widely in vacuum, creating a considerable flow in the backward direction. Some major effects from the plume could include contamination from mass deposition, unsatisfactory disturbance torques, and surface heating.

To gain a better understanding of thruster-satellite interaction and design considerations in placing electric propulsion on satellites, a study of small thruster plumes is currently in progress. Of particular interest is the prediction of plume expansion in vacuum, especially in the off-axis region that may affect spacecraft surfaces. The problem is being approached numerically, by

[†] Aerospace Engineer, Member AIAA

[‡] Research Scientist, Member AIAA

^{*} Graduate Student

[§] Professor Chem. Engr., Member AIAA

modeling the nozzle flow and plume on both the continuum and molecular level, and experimentally by making plume flow-field measurements in a vacuum facility. One aspect of the overall study is to examine the fluid mechanics of transition, near-rarefied, and rarefied flow regimes. A second is to assess the effectiveness of molecular-level models in predicting low-density expanding flows and determine the applicable range of the continuum formulation for these flows. A third is to provide experimental verification of the numerical methods. Addressed specifically in this paper is experimental verification of a molecular-level model in the plume of a nitrogen nozzle flow.

It is interesting to compare the current experimental investigation with similar studies performed previously on small control thrusters. In the DFVLR vacuum facility in Gottingen, Germany, Legge and Dettleff¹ made Pitot pressure measurements in the plume of a small hydrazine thruster to an axial distance of 100 mm. In the CNRS vacuum facility in Meudon, France, Lengrand et al.² obtained density and rotational temperatures using an electron beam in the plume of a nitrogen thruster to a distance of 240 mm. More recently, Jafry and Vanden Beukel³ made mass-flux measurements in a helium plume of a small thruster to a distance of 140 mm. For the current investigation, the measurement distance in the plume is nearly double that of the maximum extent reported in these studies.

From recent investigations in the current study, the flow of carbon dioxide⁴ and nitrogen⁵ in a nozzle were computed with two numerical techniques based on the different physical approaches. The technique based on continuum theory numerically solved the Navier-Stokes equations for compressible flow. The other technique, based on a stochastic model of kinetic theory, used the direct simulation Monte Carlo (DSMC) method. Both methods were applied to solution of a low-density, viscous gas flow in a converging-diverging nozzle of conical shape. The continuum solution started in the converging section of the nozzle and was carried through to the exhaust plane. The computational domain for the DSMC method started slightly downstream of the nozzle throat and extended into the plume about one nozzle diameter. The inflow conditions for the DSMC method were provided by the

continuum solution. The solutions from the two methods exhibited differences, mainly in the region near the wall at the nozzle lip. The work described in References 4 & 5 demonstrated that the numerically intensive DSMC technique could be applied readily to a low-density nozzle flow, where the flow varied from continuum at the throat to rarefied at the exit plane. Furthermore, the DSMC results were successfully validated by experimental measurements made in the near-field plume in an area extending 1.1 nozzle diameters (36 mm) axially and 0.8 diameters (24 mm) radially.⁵

In continuation of the study, computational and experimental results were recently obtained for a larger portion of the nitrogen plume than was reported in Reference 5 and are reported in this paper. As in the work reported in Reference 5, experimental measurements were made specifically for validation of the numerical studies. The experimental work was conducted using the same vacuum facility and apparatus that simulated the flow of a small thruster. In this part of the investigation, a new traverse mechanism was used that allowed for the increased measurement area in the plume. New also in this investigation were measurements of flow angle made with a conical probe and Pitot pressures made with an impact tube appropriately sized for the density and flow velocity of the far-field plume. The measurement area in this study extended to nearly 16 nozzle diameters (460 mm) in the axial direction, downstream of the nozzle exhaust plane, and 2 diameters (60 mm) in the radial direction perpendicular to the plume axis. The unique nature of this extended test range allowed evaluation of the numerical method for very rarefied flow conditions.

For the work reported in this paper, the DSMC simulation was performed only for the plume. For this case the inflow surface was the exhaust plane of the nozzle and the conditions were obtained from the previous simulation of the nozzle flow. The plume simulation required about an order of magnitude less CPU time than the simulation of the nozzle flow, proportional to the difference in density between the two flow regions. In this part of the study, results from the DSMC simulation of the plume helped guide the experimental work in selection of Pitot probe size and interpretation of flow angle measurements.

This paper presents a description of the experimental apparatus used in the current investigation, a brief discussion of the numerical simulation, and comparisons of experimental measurements with results computed from the DSMC method.

Reference Configuration

The nozzle configuration selected for both experimental and computational study simulates the viscous flow of an electric propulsion device. The nozzle consisted of a conical geometry for simplicity of both numerical modeling and machining, but is also a typical shape for small thrusters. The nozzle is illustrated in Figure 1, with geometrical details given in Table 1. The experimental operating conditions for the nozzle are given in Table 2.

For laboratory and computational convenience, nitrogen was used for the test gas and does not particularly represent the actual propellant of a spacecraft propulsion system. A flow rate of 6.8×10^{-5} kg/s was chosen to match the pumping capacity of the vacuum system on the experimental facility. For this flow rate, the nozzle was sized to provide similarity of the Reynolds Number with an actual electrothermal thruster. The nominal Reynolds Number of 850 listed in Table 2 is based on throat diameter and viscosity of the nitrogen at the stagnation temperature of 700 K. This Reynolds Number is characteristic of a high-temperature resistojet or arcjet. For these conditions, flow at the throat was in the continuum regime, as indicated by the Knudsen Number of 2×10^{-3} (also based on throat diameter), but reached near-rarefied at the nozzle exhaust plane.

Vacuum Facility

The experimental work for this study was conducted in a vacuum tank for space-simulation tests. The test apparatus was mounted in a 1 m diameter section about 1 m in length that is attached to a larger tank about 4.9 m in diameter and 19 m long. The test section and tank are evacuated by a vacuum system consisting of twenty oil-diffusion pumps in series with four blowers and four roughing pumps. A detailed

description of the test facility can be found in Reference 6.

The pumping system was able to maintain a vacuum of about 2×10^{-2} Pa for a nozzle flow rate of 6.8×10^{-5} kg/s. The vacuum pressure was monitored with a hot-cathode ionization gauge mounted on the 1 m diameter test section.

Experimental Apparatus

The apparatus used in this study to simulate a thruster was previously described in Reference 5 as the design denoted Configuration 2 and is shown schematically in Figure 2. In this design the nitrogen was heated to a temperature of 700 K in an annular area comprised of a 12.7 mm diameter cartridge heater contained in a tube 17.3 mm in internal diameter. The stagnation pressure and temperature of the flow were measured upstream of the nozzle in a 22.1 mm diameter plenum. The pressure was measured with a capacitance manometer having a full-scale range of 13.3 kPa and a listed accuracy of 1% of reading. The gas temperature was measured with a half-shielded, chromel-alumel thermocouple with the hot junction located at the centerline of the measurement station and connected to a digital voltmeter with self-contained, cold-junction compensation. The flow rate of nitrogen was measured with a commercially available thermal-conductivity type flow meter. The flow was regulated with a controller consisting of a flow meter of similar type and a feedback loop to an electrically operated valve. A schematic of the flow system is shown in Figure 3. The flow meter and controller were both calibrated in place on the test apparatus by timing the flow of nitrogen into a known volume and recording the temperature and pressure of the volume before and after the timed period to determine a flow rate. The accuracy of the flow readings for all experimental tests is estimated to be within $\pm 2\%$.

A traversing mechanism was used for making measurements in the nozzle plume. The mechanism consisted of a rotary-traverse table mounted atop two linear-traverse tables, with travel axes mutually perpendicular to provide movement in the radial, axial and rotational directions. The range of travel was 280 mm in the radial (R) direction, 480 mm in the axial (Z) direction, and

360 degrees in rotation. The tables were driven with stepping motors operated from a microprocessor control panel. Position of traverse was monitored by encoders mounted on each table. The zero position of travel was established for each probe by positioning the probe tip at the center point of the nozzle exit plane and aligning the probe with the axis of the nozzle. Positional accuracy of the traverse tables was within ± 0.12 mm over the maximum extent of the axial measurement range and $\pm 1.5 \times 10^{-2}$ mm over the radial range. The repeatability of probe position from one test to another was limited to the uncertainty in the initial positioning of the probe and is estimated to be within ± 0.5 mm in both the axial and radial directions.

Measurement Probes

Two types of intrusive probes were used to make measurements in the plume. Pitot tubes were used to measure total pressure and a conical probe was used to measure flow angle. Pitot tubes with diameters of 1 mm and 6.4 mm were used, each in a particular region of the flow to maintain a useful range of probe Reynolds Number for applying a correction to shock strength for rarefaction effects. This correction is described in a later section. The 1 mm diameter tube was attached to a 1.3 kPa full-scale capacitance manometer with a three decade measurement range and a listed manufacturer's accuracy of 1% of reading. The 6.4 mm tube was used with a 133 Pa full-scale capacitance manometer having a three decade range and a listed accuracy of 0.25% of reading. The measurement uncertainty of the Pitot tubes depended on position in the flow field, mainly due to pressure gradients, and is estimated to vary between a maximum of $\pm 9\%$ at the nozzle exit plane for the 1 mm tube to a minimum of $\pm 2\%$ in the far-field for the 6.4 mm tube.

The probe of conical shape used to measure flow angle in the plume was 6.4 mm in diameter at the base of a 30 degree cone. Two 1 mm static taps were located on opposite sides of the cone as shown in Figure 4. Each tap was connected to an individual capacitance manometer with a full-scale range of 133 Pa as previously described. To obtain flow angle, the probe was rotated in the stream until the readings on the static taps were

equalized. This rotational angle was taken as the flow angle for the particular location of the probe tip in the plume, assuming that the shock and static pressure behind the shock on the cone surface were symmetrical when the cone was aligned with the stream. A typical rotary scan with the conical probe at an axial station 60 mm from the nozzle exit plane and a radial position 30 mm from the nozzle axis is shown in Figure 5. The figure shows plots of the pressure for each static tap as a function of the rotation angle, where the rotation angle is referenced to the plume axis. As can be seen in the figure, the static pressures on the cone were fairly sensitive to the angle of the probe in the stream and the slopes of the lines differed depending on whether the tap was directed into the oncoming flow or in the wake of the flow. The accuracy of this probe is dependent on the pressure gradient in the stream (i.e. the pressure difference across the taps) and is more accurate in the far-field of the plume where the gradients are low. In the far-field, the measurement uncertainty is estimated to be within $\pm 1^\circ$. A more detailed description of measurement uncertainty for the probe data is contained in Reference 7.

All reported flow angles and Pitot pressures were taken in the horizontal plane of the nozzle. Previous tests demonstrated nearly exact symmetry of the plume in the horizontal and vertical planes.

Test Procedure

The test section containing the experimental apparatus was first evacuated without flow and the capacitance manometers zeroed. The vacuum pressure without flow was about 1×10^{-4} Pa which served as the zero-reference pressure for the manometers. The flowmeter was zeroed while containing nitrogen at the accumulator supply pressure. After all instrumentation was zeroed, flow was established at 6.8×10^{-5} kg/s and maintained by the flow controller. Simultaneously, about 65 Watts was applied to the heater and time allowed for the system to equilibrate at a nozzle-inlet temperature of 700 K.

On attaining steady conditions, surveys were taken by positioning the particular measurement

probe in the plume with the traverse mechanism. Probe position was maintained until capacitance manometer readings reached a steady condition. Generally, measurements of Pitot pressures were preceded by measurements of flow angle in the far-field of the plume ($Z > 60$ mm). In this manner, the 6.4 mm diameter Pitot tube was immediately positioned at the angle of the flow for a reading. In the near-field of the plume, flow angles were made with both the conical probe and the 1 mm Pitot tube.

DSMC Computation of Plume Flow

The direct simulation Monte Carlo method (DSMC) has previously been evaluated successfully for expanding flows for the near-field plume of a nitrogen thruster⁵ and in the far-field plume of a helium thruster.⁸ In Reference 5 the DSMC method was applied to the internal nozzle flow with the computational domain starting slightly downstream of the nozzle throat and applying the results of a continuum solution for the inflow conditions. In the current application, the computation was begun at the nozzle exit plane using the DSMC simulation data generated previously as described in Reference 5. The expansion was assumed to occur in a pure vacuum.

A computational grid was generated in which the cell dimensions were scaled with an assumed profile for the decay in density away from the nozzle exit. Densities from the previous solution were used in the near-field to about 36 mm and a $1/r^2$ relation in the remainder of the field. A computational domain covering 500 mm by 300 mm was spanned with 5280 cells, 88 axially and 60 radially. An average of 55 particles per cell was employed in the simulation. Macroscopic flow quantities were obtained by averaging over 2000 time-steps after a transient period of 1000 iterations. The total computational time of the simulation using a vectorized code was 750 CPU seconds on a Cray Y/MP.

Results from the DSMC method are given in Figure 6. Figure 6a is a contour plot of Mach Number for the computational domain extending radially 300 mm and axially by 500 mm. The flow emanates from the nozzle in the lower left-hand corner of the figure. The Mach number at

the centerline of the nozzle exit plane is about 5 and increases to over 16 at the far downstream end of the domain. Figure 6b is a contour plot of the stream pressure on a logarithmic scale in the plume for the same domain. The pressure decreases by about 3 orders of magnitude along the plume axis 500 mm from the nozzle exit plane.

Calculation of Pitot Pressure

To compare the numerical solution with the experimental Pitot tube data, Pitot pressures were first calculated from the numerical results using the computed values of static pressure, Mach Number and density. The procedure for computing the Pitot pressure is detailed in Reference 5 and in summary includes:

1. Calculating the ideal pressure ratio across a normal shock with the Rayleigh Pitot tube equation, and;
2. Obtaining probe pressure by correcting for shock strength in a rarefied stream.

The relation for the rarefaction correction to shock strength was obtained from parametric curves presented in Reference 9. The curves were correlations of experimental measurements made in rarefied wind tunnel flows and are given as a function of Reynolds Number based on probe diameter. The corrections were limited to a range of probe Reynolds Number > 0.5 . To stay within the useful range of the correction, the probe diameter was either 1 mm or 6.4 mm depending on the region of measurement in the plume. The appropriate probe size for a particular region was obtained from a contour plot of probe Reynolds Number generated with the flow properties from the DSMC solution using a 1 mm characteristic diameter. The contour plot is given in Figure 7. The 6.4 mm tube was used in the region bounded by the Reynolds Number contour of 0.1 and the 1 mm tube was used in the inner region bounded by the contour for 1.

Experimental and Computed Results

Measured and computed flow angles are compared in the contour plot of Figure 8. Con-

tours of the flow angle computed by the DSMC simulation are given in the upper half of the figure and measurements in the bottom half. In this figure each line is an isogram of flow angle referenced to the nozzle axis. The contours originate at a point 12 mm downstream of the nozzle exhaust plane, and the nozzle axis is at the radial distance of zero. The blank, stepped sections in the bottom left portion of the plot are areas in the plume where the pressure signals from the static taps were too low to make measurements. The plot illustrates the qualitative agreement between measured and computed values of the flow angle over a large portion of the measurement area and also illustrates the manner by which the flow fans out into the vacuum.

There is some discrepancy in the flow angle in the near-field of the plume which is more clearly illustrated in Figure 9a. In this figure, flow angles obtained from the DSMC simulation, the conical probe, and data taken previously by rotating the 1 mm Pitot tube in the flow⁵ are plotted with radial distance from the plume axis at the axial station 12 mm from the nozzle exit plane. There is a fairly large difference in the angles obtained from the conical probe and the DSMC results at radial distances between about 5 to 20 mm ($R/De = 0.2$ to 0.6). In this region, the pressure gradient in the stream is quite high and is illustrated with results generated from the DSMC simulation in Figure 10 by the solid line. Also, at this location ($Z/De = 0.38$), the probe is quite large with respect to the nozzle exit diameter. The large difference in the angles may be a consequence of flow distortion by the probe and the difference in stream pressure over the separation distance of the static taps from the steep gradient. The 1 mm Pitot tube data agrees more closely with the DSMC results and shows the possible effect of probe size.

The comparison between measured and computed angles improves the further away from the nozzle the data was obtained. Figure 9b compares conical probe measurements and DSMC results at a location 160 mm ($Z/De = 5$) downstream of the nozzle exit. Here the agreement between measured and computed values is within 4%. At this location, flow distortion from the probe would be minimal and pressure gradients in the stream low as suggested by the lower dashed line in Figure 10

which is the stream pressure at an axial station of 100 mm.

Figure 11 compares Pitot pressures as measured and computed from the DSMC results along the plume axis on a semi-log plot. The plot extends from the nozzle exit plane to a normalized axial distance of 15 (480 mm). In this range, the pressure drops by two orders of magnitude. This plot combines data from the 1 mm probe that spanned the axial range of 0 to 1.1 (36 mm) and the 6.4 mm probe that spanned 0.6 to 15 (18 mm to 480 mm). Where data from the two probes overlapped, the measurements were nearly identical. As seen from the plot, the agreement between measured and computed results is slightly better in the higher pressure region of the near-field, but is generally quite good over the entire range.

Far-field pressure measurements are now considered in more detail. A comparison of measured and computed Pitot pressures is presented in the contour plot of Figure 12 for the measurement area extending from $Z = 60$ mm to 160 mm and for $R = 0$ to 60 mm. In this region of the plume, the measurements were made with the 6.4 mm diameter Pitot tube. In Figure 12, the pressures computed from the DSMC results, including the rarefaction correction, are plotted in the top half and the measured pressures in the bottom half. The lines represent isobars of Pitot pressure. On the plume axis ($R = 0$), the pressures computed from the DSMC results are about 10% higher than the measured values. Away from the plume axis, the agreement improves as is shown more definitively in the semi-log plots of Figure 13. Plotted in Figure 13a are measured and computed Pitot pressures from the plume axis to a radial distance of 60 mm ($R/De = 1.9$) at the axial station 60 mm from the nozzle exhaust plane. Figure 13b is a plot for the same radial scan at the axial station 160 mm from the exhaust plane. As shown in the figures, the agreement between measured and computed values of the Pitot pressure is quite good over a large portion of the radial distance, with the computed value of Pitot pressure falling below the measured value at the outer extent of the radial scan.

In the DSMC simulation the plume was assumed to expand into a perfect vacuum whereas in

the experimental facility the plume actually expands into a back pressure of about 2×10^{-2} Pa. This difference may account for the discrepancy between measured and computed pressure profiles in the outer, lower pressure regions of the plume in Figure 13. This aspect of the problem will be investigated in later studies by inclusion of the actual vacuum facility back pressure in the DSMC simulation.

Concluding Remarks

The experimental tests were designed specifically as a model problem for verification of the DSMC method applied to an expanding nozzle flow as originally described in Reference 5. This paper described the continuation of that work, whereby a larger portion of a nitrogen plume from a conical nozzle was computed with the DSMC method and compared to measurements. The measurements consisted of Pitot pressures made with two different sized tubes and flow angles made with a conical probe. The agreement between measured and computed values of the Pitot pressure were generally quite good, with Pitot pressure comparisons showing closer agreement in the higher pressure regions of the plume. Flow angle comparisons showed closer agreement in the far-field. Conical probe size is thought to be a primary factor for the discrepancy between the measured and computed values of flow angle made in the near-field plume.

The generally good agreement between the measured and computed results from this study further verifies the validity of the DSMC method in calculation of expanding flows. Furthermore, the total computational time of 750 CPU seconds demonstrates the relative efficiency of the DSMC method for such calculations.

A somewhat unique aspect of this study was the mutual benefit of experimental and numerical results. On the one hand, the experimental measurements verified the usefulness of the DSMC method for simulating low-density, expanding flow. On the other, the DSMC results were used to determine appropriate Pitot probe size for specific regions of the plume to maintain a useful range of the available relationship for the rarefaction correction and also helped interpret the flow

angle measurements made with the conical probe.

References

1. Legge, H. and Dettleff, G., "Pitot Pressure and Heat Transfer Measurements in Hydrazine Thruster Plumes," *J. Spacecraft and Rockets*, Vol. 23 (4), July 1986, pp. 357-362.
2. Lengrand, J.C., Allegre, J., and Raffin, M., "Experimental Investigations of Underexpanded Thruster Plumes," *AIAA Journal*, Vol. 14, (5), May 1976, pp. 692-694.
3. Jafry, Y. and Vanden Beukel, J., "Ultralow Density Plume Measurements Using a Helium Mass Spectrometer," *J. Vacuum Science and Technology* (in press).
4. Boyd, I.D., Penko, P.F., and Carney, L.M., "Efficient Monte Carlo Simulation of Rarefied Flow in a Small Nozzle," AIAA Paper 90-1693, June 1990.
5. Boyd, I.D., Penko, P.F., Meissner, D.L., and DeWitt, K.J., "Experimental and Numerical Investigations of Low-Density Nozzle and Plume Flows of Nitrogen," *AIAA Journal* (in press).
6. Finke, R.C., Holmes, A.D. and Keller, T.A., "Space Environment Facility for Electric Propulsion Systems Research," NASA TN-D-2774, 1965.
7. Meissner, D.L., M. Sc. Thesis, University of Toledo, Toledo, Oh, 1992 (in progress).
8. Boyd, I.D., Jafry, Y., and Vanden Beukel, J., "Investigation of Nozzle and Plume Expansions of a Small Helium Thruster," *18th International Symposium on Rarefied Gas Dynamics*, July 1992.
9. Stephenson, W.B., "Use of the Pitot Tube in Very Low Density Flows," AEDC-TR-81-11, Oct. 1981.

Table 1: Nozzle Geometry

Throat Diameter, D_t	3.18 mm
Exit Diameter, D_e	31.8 mm
Inlet Diameter, D_i	22.1 mm
Wall thickness, t_w	1.65 mm
Area Ratio (Exit / Throat)	100
Inlet half-angle, θ_i	45°
Exit half-angle, θ_e	20°

Table 2: Nozzle Test Conditions

Propellant	N_2
Flow Rate	6.8×10^{-5} kg/s
Total Pressure, P_o	6210 Pa
Total Temperature, T_o	700 K
Wall Temperature, T_{w1}	507 K
Wall Temperature, T_{w2}	498 K
Throat Reynolds Number	850
Throat Knudsen Number	2×10^{-3}

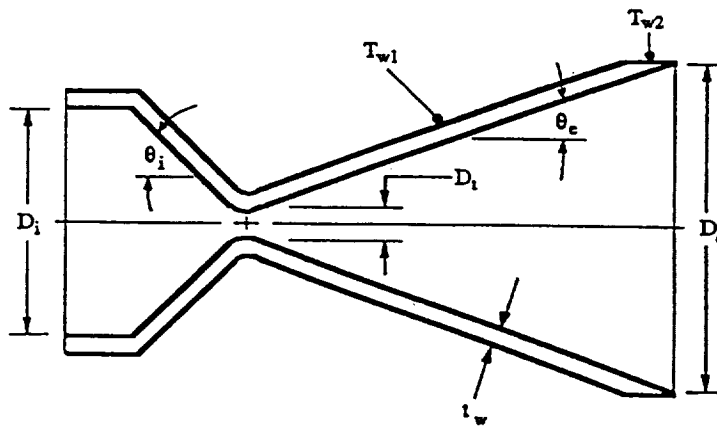


Figure 1. Nozzle Diagram

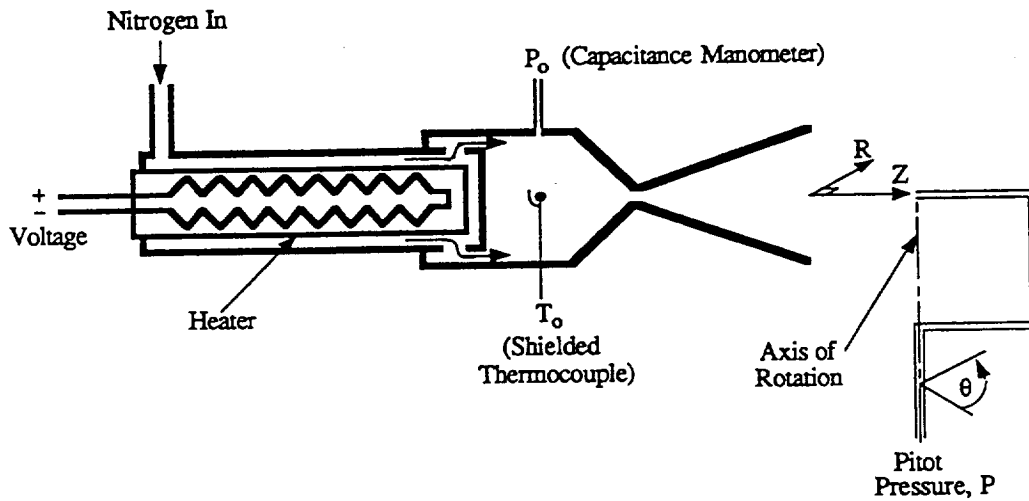


Figure 2. Schematic of Simulated Thruster

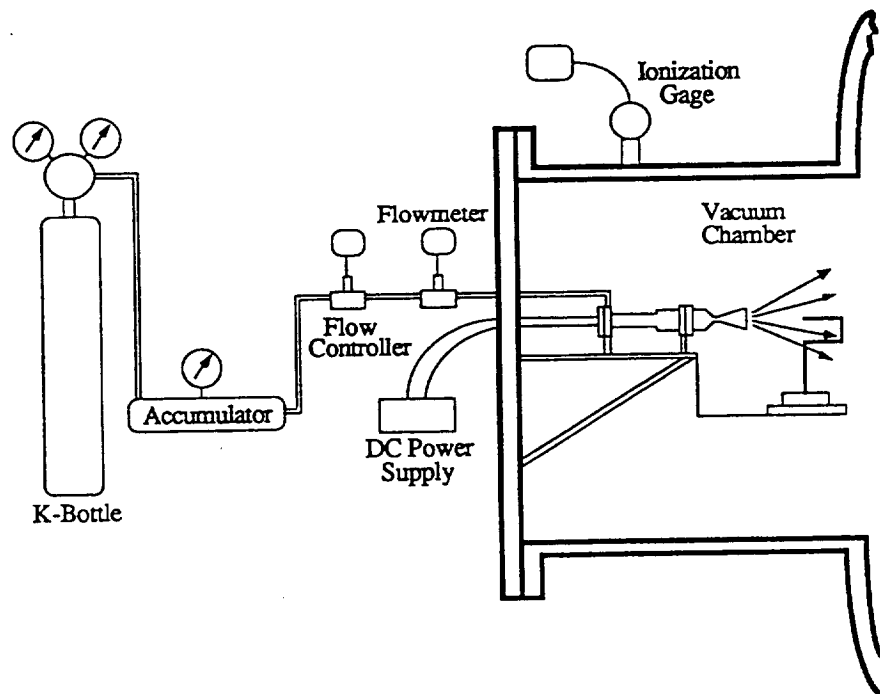


Figure 3. Schematic of Experimental Facility

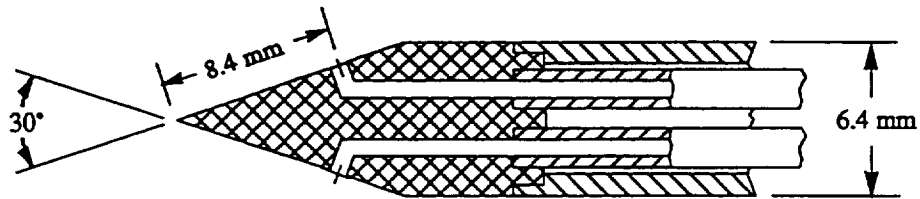


Figure 4. Cross-Sectional Schematic of Conical Probe

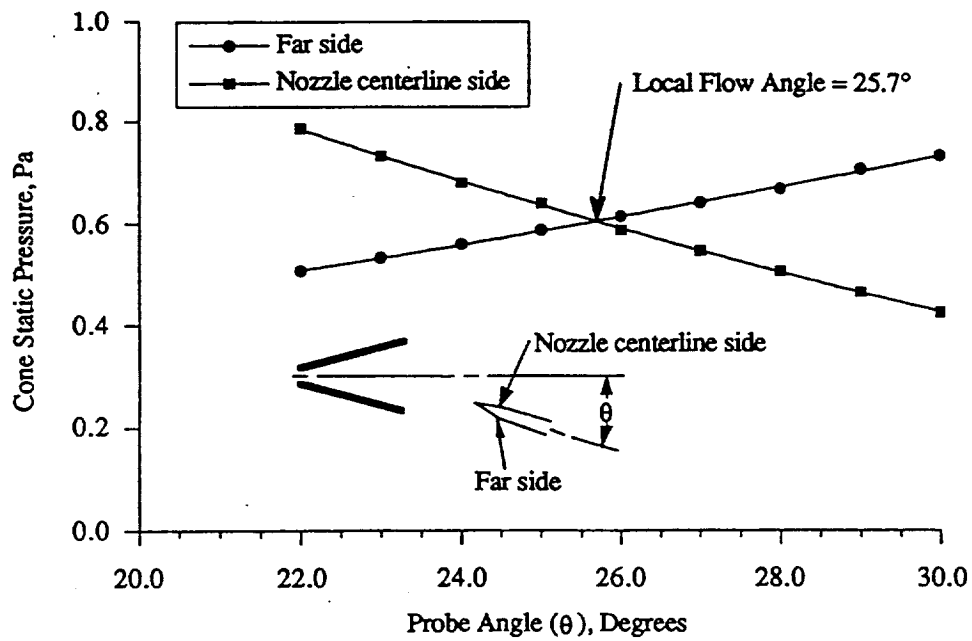


Figure 5. Static Pressure vs. Rotation Angle for the Conical Probe at $Z = 60$ mm ($Z/D_e = 1.89$) and $R = 30$ mm ($R/D_e = 0.94$).

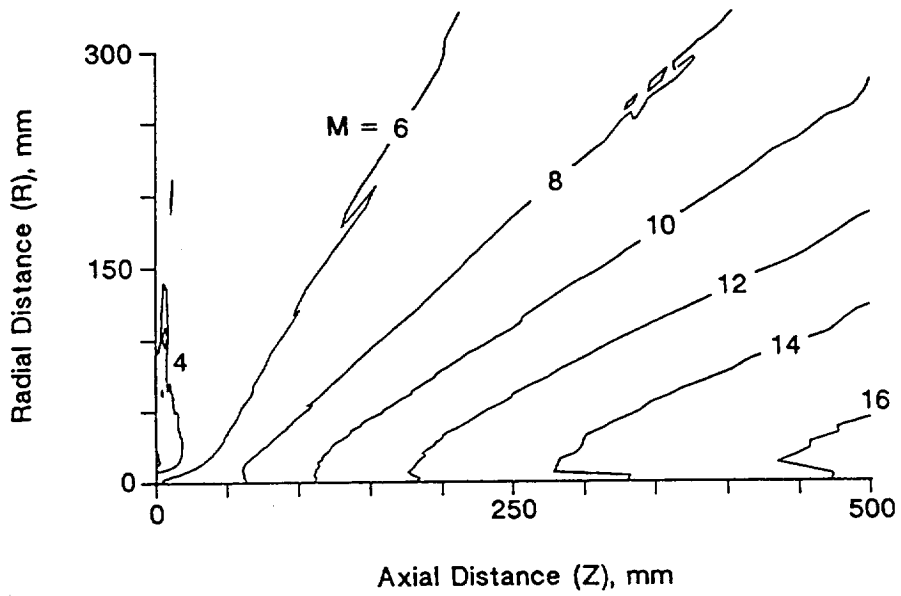


Figure 6a. Mach Number Contours in the Plume from the DSMC Simulation.

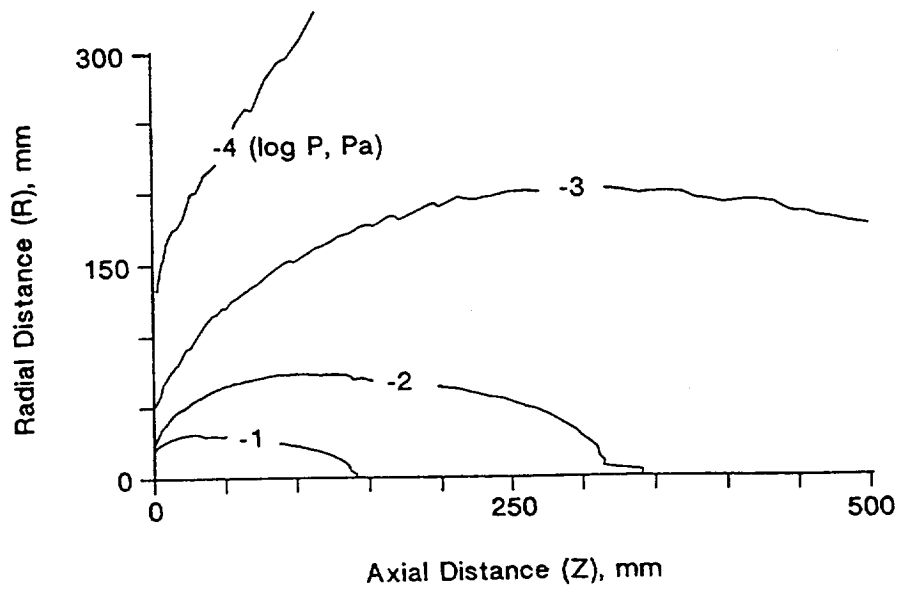


Figure 6b. Contours of Logarithm of Pressure in the Plume from the DSMC Simulation.

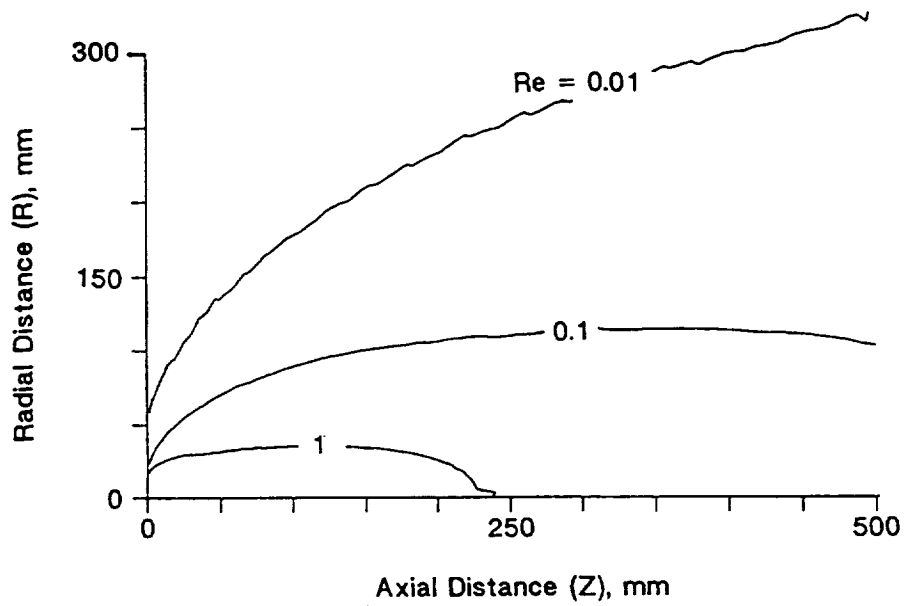


Figure 7. Contours of Logarithm of Probe Reynolds Number for a 1 mm Characteristic Diameter Computed from the DSMC Results.

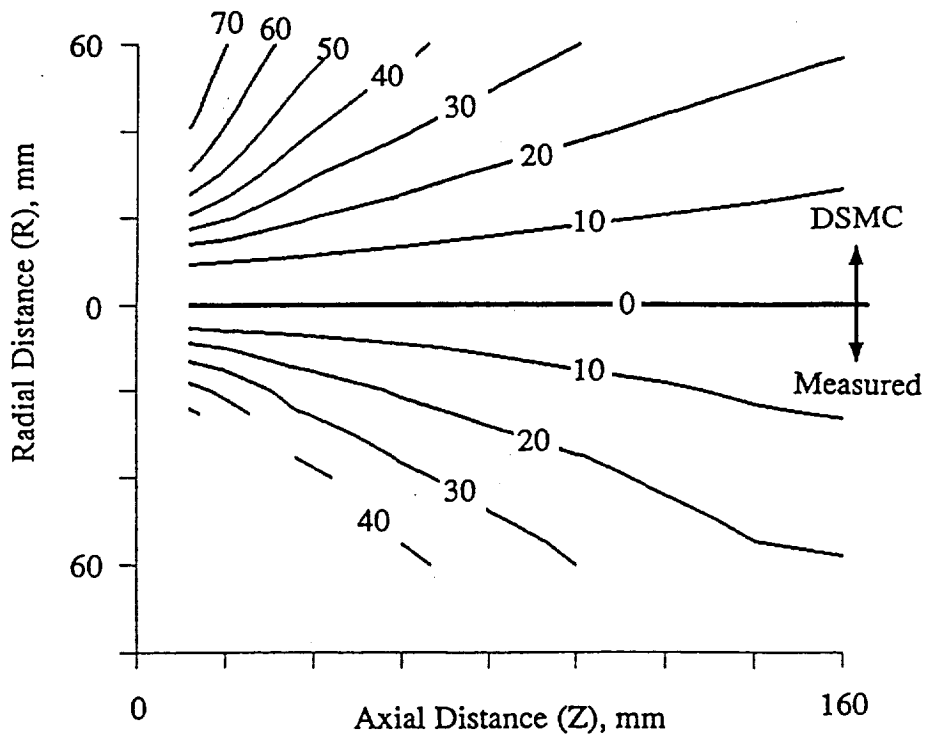


Figure 8. Contours of Flow Angle, Measured and from the DSMC Simulation Starting 12 mm from the Nozzle Exhaust Plane. Top half: DSMC. Bottom half: Measured.

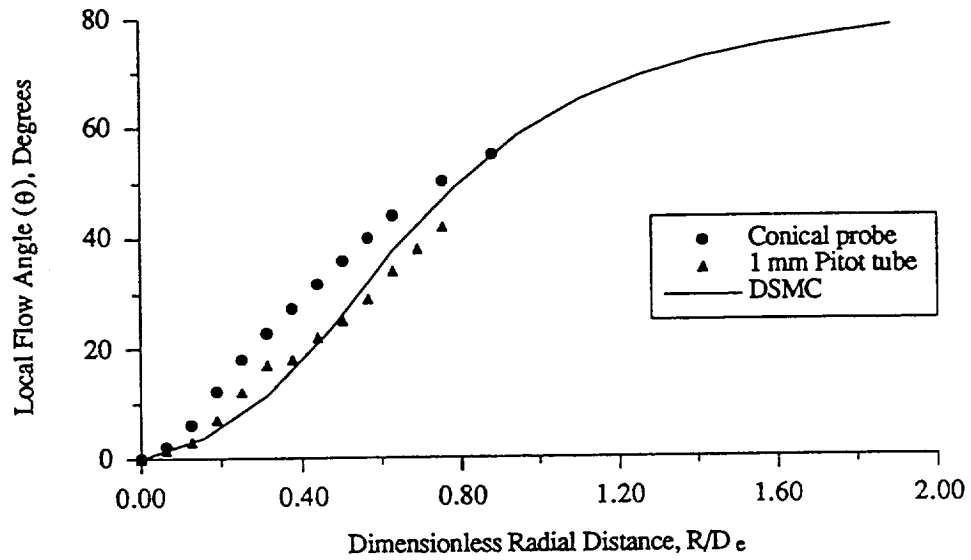


Figure 9a. Measured and DSMC Flow Angles for a Radial Scan at the Axial Station $Z = 12 \text{ mm}$ ($Z/D_e = 0.38$).

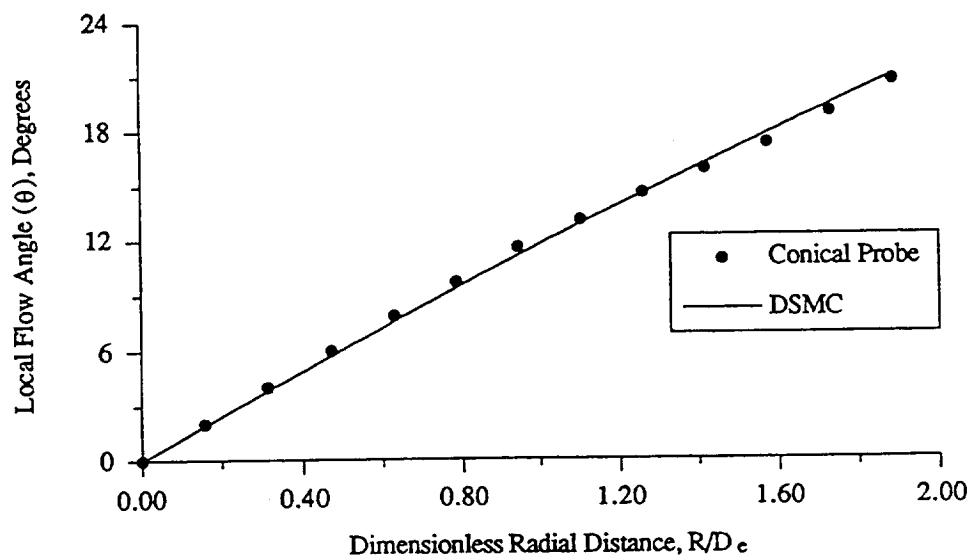


Figure 9b. Measured and DSMC Flow Angles for a Radial Scan at the Axial Station $Z = 160 \text{ mm}$ ($Z/D_e = 5.04$).

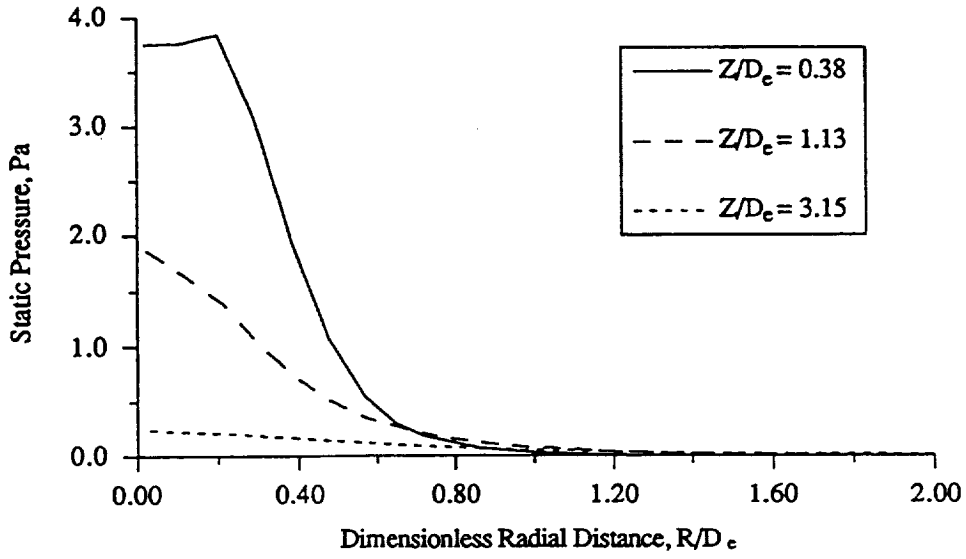


Figure 10. Stream Pressures from the DSMC Simulation for the Axial Stations $Z = 12$ mm ($Z/D_e = 0.38$), 36 mm ($Z/D_e = 1.13$) & 100 mm ($Z/D_e = 3.15$).

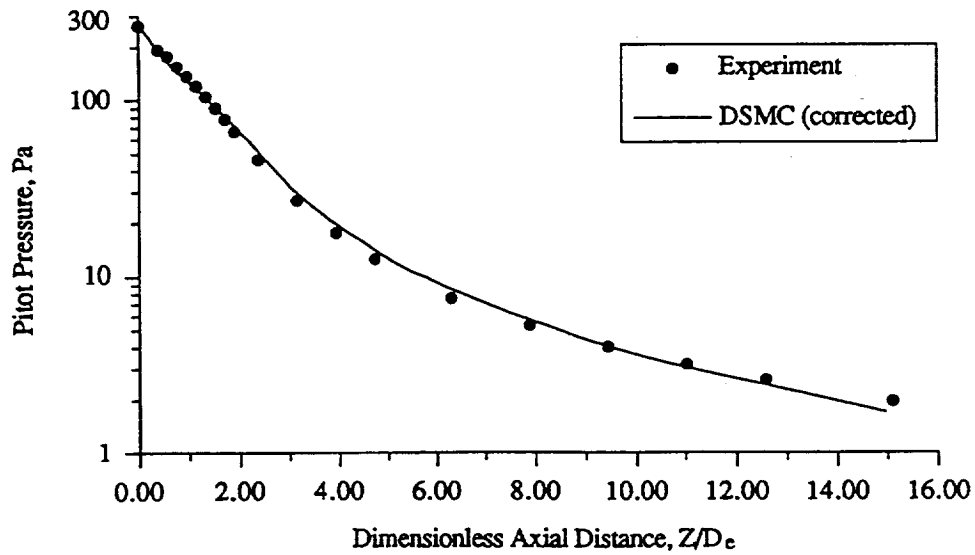


Figure 11. Comparison of Experimental and Computed Values of the Pitot Pressure Along the Plume Axis.

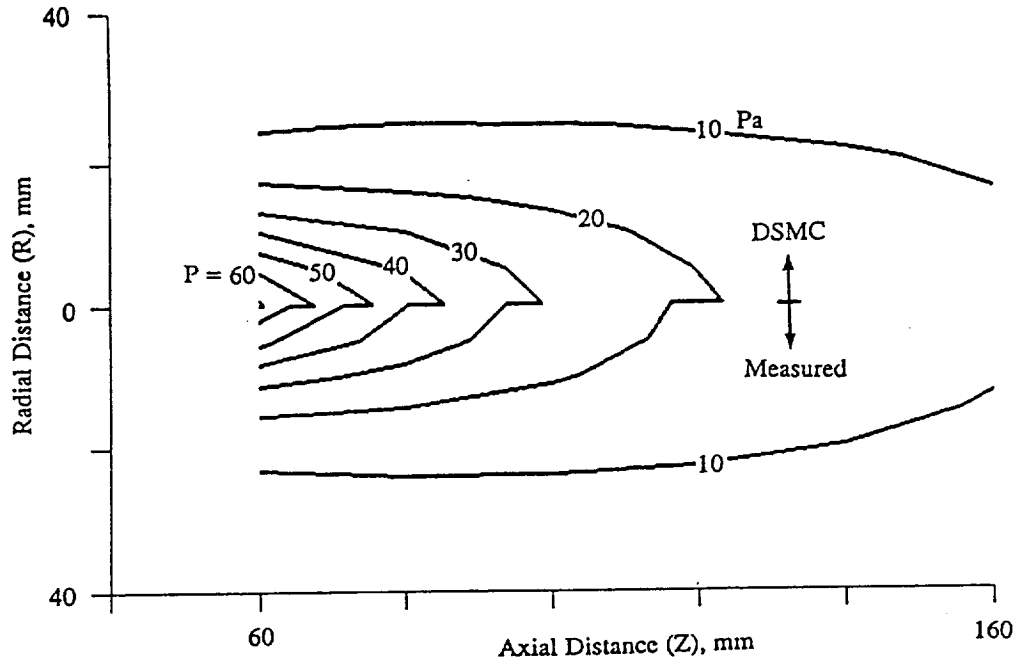


Figure 12. Contours of Pitot Pressure (Pa) Computed from the DSMC Simulation and as Measured for the Area $Z = 60$ mm to 160 mm and $R = 0$ to 40 mm. Top half: DSMC. Bottom half: Measured.

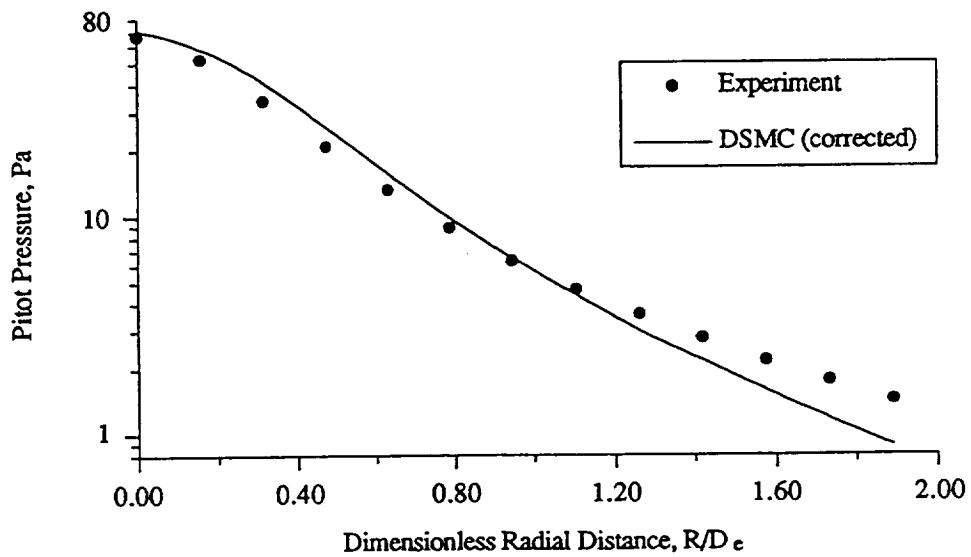


Figure 13a. Pitot Pressures as Measured and Computed from the DSMC Simulation for a Radial Scan at the Axial Station $Z = 60$ mm ($Z/D_e = 1.89$).

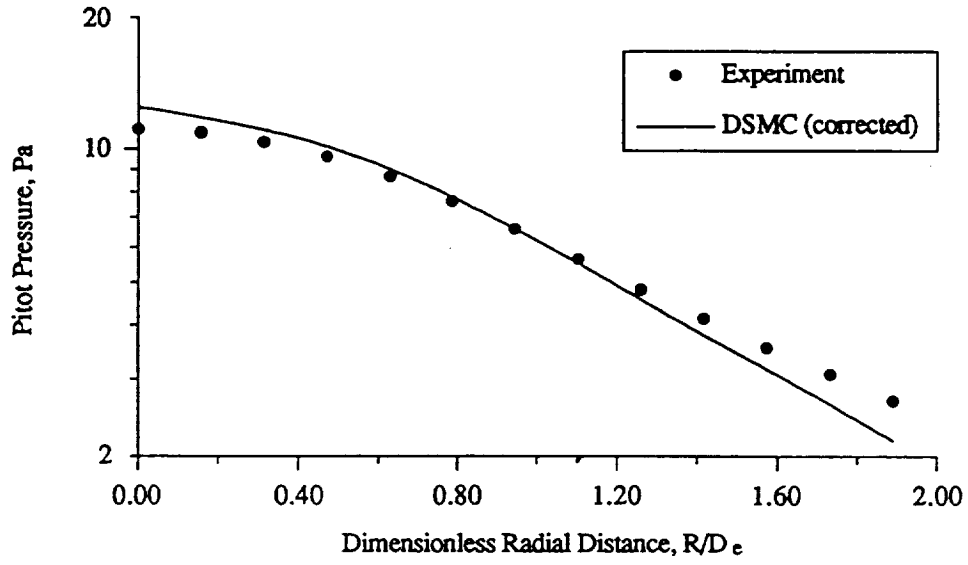


Figure 13b. Pitot Pressures as Measured and Computed from the DSMC Simulation for a Radial Scan at the Axial Station $Z = 160$ mm ($Z/D_e = 5.04$).

REPORT DOCUMENTATION PAGE

Form Approved
OMB No. 0704-0188

Public reporting burden for this collection of information is estimated to average 1 hour per response, including the time for reviewing instructions, searching existing data sources, gathering and maintaining the data needed, and completing and reviewing the collection of information. Send comments regarding this burden estimate or any other aspect of this collection of information, including suggestions for reducing this burden, to Washington Headquarters Services, Directorate for Information Operations and Reports, 1215 Jefferson Davis Highway, Suite 1204, Arlington, VA 22202-4302, and to the Office of Management and Budget, Paperwork Reduction Project (0704-0188), Washington, DC 20503.

1. AGENCY USE ONLY (<i>Leave blank</i>)	2. REPORT DATE April 1993	3. REPORT TYPE AND DATES COVERED Technical Memorandum	
4. TITLE AND SUBTITLE Measurement and Analysis of a Small Nozzle Plume in Vacuum		5. FUNDING NUMBERS WU-506-42-31	
6. AUTHOR(S) P.F. Penko, I.D. Boyd, D.L. Meissner, and K.J. DeWitt			
7. PERFORMING ORGANIZATION NAME(S) AND ADDRESS(ES) National Aeronautics and Space Administration Lewis Research Center Cleveland, Ohio 44135-3191		8. PERFORMING ORGANIZATION REPORT NUMBER E-7383	
9. SPONSORING/MONITORING AGENCY NAMES(S) AND ADDRESS(ES) National Aeronautics and Space Administration Washington, D.C. 20546-0001		10. SPONSORING/MONITORING AGENCY REPORT NUMBER NASA TM-106066 AIAA-92-3108	
11. SUPPLEMENTARY NOTES Prepared for the 28th Joint Propulsion Conference and Exhibit cosponsored by the AIAA, SAE, ASME, and ASEE, Nashville, Tennessee, July 6-8, 1992. P.F. Penko, NASA Lewis Research Center; I.D. Boyd, Eloret Institute, NASA Ames Research Center, Moffett Field, California; D.L. Meissner and K.J. DeWitt, University of Toledo, Toledo, Ohio. Responsible person; Paul F. Penko, (216) 977-7490.			
12a. DISTRIBUTION/AVAILABILITY STATEMENT Unclassified - Unlimited Subject Category 20		12b. DISTRIBUTION CODE	
13. ABSTRACT (<i>Maximum 200 words</i>) Pitot pressures and flow angles are measured in the plume of a nozzle flowing nitrogen and exhausting to a vacuum. Total pressures are measured with Pitot tubes sized for specific regions of the plume and flow angles measured with a conical probe. The measurement area for total pressure extends 480 mm (16 exit diameters) downstream of the nozzle exit plane and radially to 60 mm (1.9 exit diameters) off the plume axis. The measurement area for flow angle extends to 160 mm (5 exit diameters) downstream and radially to 60 mm. The measurements are compared to results from a numerical simulation of the flow that is based on kinetic theory and uses the direct-simulation Monte Carlo (DSMC) method. Comparisons of computed results from the DSMC method with measurements of flow angle display good agreement in the far-field of the plume and improve with increasing distance from the exit plane. Pitot pressures computed from the DSMC method are in reasonably good agreement with experimental results over the entire measurement area.			
14. SUBJECT TERMS Nozzle plume; Pitot pressure; Direct-simulation Monte Carlo; Rarefied flow		15. NUMBER OF PAGES 18	
		16. PRICE CODE A03	
17. SECURITY CLASSIFICATION OF REPORT Unclassified	18. SECURITY CLASSIFICATION OF THIS PAGE Unclassified	19. SECURITY CLASSIFICATION OF ABSTRACT Unclassified	20. LIMITATION OF ABSTRACT

National Aeronautics and
Space Administration

Lewis Research Center
Cleveland, Ohio 44135

Official Business
Penalty for Private Use \$300

FOURTH CLASS MAIL

ADDRESS CORRECTION REQUESTED



NASA

